Supplement Information

Physical and chemical characterisation of PM emissions from two ships operating in European Emission Control Areas

Moldanová, J., Fridell, E., Winnes, H. , Holmin-Fridell, S., Boman, J., Jedynska, A., Tishkova, V., Demirdjian, B., Joulie, S., Bladt, H., Ivaleva, N., P., Niessner, R.

Table S1. Properties of the investigated ships

Ship	Type	Length [m]	Gross tonnage	Built year	Max/average speed [knots]
S1	Dry cargo	166	18 773	1987	14.9/13
S2	RoPax Ferry	240	46 353	2001	21.5/17.7

Table S2. Engine parameters for the campaign experiments. S1, S2: ships investigated, HFO1%, HFO0.5%: HFO used by engine with approximate fuel sulphur content, ME-full, ME-low: main engine with full and low

Measurement/ Engine parameter	S1_ HFO1% _ME-full	S1_ HFO1% _ME-low	S1_ MGO _AE	S2_ HFO1% _ME-full	S2_ HFO0.5% _ME-full	S2_ MGO_ ME-full
Fuel consumption (kg/h)	760	257	83	648	635	619
Fuel consumption (g/kWh)	211.5	192.3	203.9	189.4	185.7	181.0
Power (kW)	3 592	1 336	405	3 420	3 420	3 420
Nominal engine speed (rpm)	750	750	1 000	510	510	510
Actual engine speed (rpm)	720	570	870	435	435	435
Gas flow in stack (nm^3/h)*	20 922	7 667	2415	16 283	16 200, 14 600	16 800
Temperature in exhaust gas (°C)	292	290	302	360	360	360

* Calculated from fuel consumption and fuel composition, normalised to 273.15 K

Table S3. Results of fuel (column 3-5) and lubricant (column 6,7) analyses. Lubricant in main engine on S1 and S2 ships were analysed.

	Unit	S1_ HFO1% _ME	S2_ HFO1% _ME	S2_ HFO0.5% _ME	S1_ MGO _AE	S2_ MGO _ME	S1_ Lub _ME	S2_ Lub _ME	Uncertainty		
									HFO	MGO	Lub
Density (15ºC)	kg/m³	977.3	988.7	943.3	834.1	846.4	908.3	927	±1.5	±0.5	±1.5
Water	% V/V	<0.10	0.14	<0.10	<0.10	<0.10	0.3	0.11	-	-	-
S	% m/m	0.91	0.96	0.58	0.03	0.1	0.53	0.92	±10%	±34%	±10%
Ash	% m/m	0.02	0.02	0.01	<0.01	<0.01	2.7	2.7	±67%	-	±1.5%
V	mg/kg	34	20	6	<1	<1	20	71	±58%	-	±41%
Na	mg/kg	8	11	7	<1	<1	20	32	±41%	-	±25%
Al	mg/kg	16	20	16	<1	<1	6	4	±34%	-	±34%
Si	mg/kg	14	18	15	<1	<1	8	18	±33%	-	±33%
Fe	mg/kg	16	9	7	<1	<1	10	25	±34%	-	±28%
Ni	mg/kg	16	15	9	<1	<1	12	60	±54%	-	±41%
Ca	mg/kg	5	8	4	<1	<1	8230	7670	±36%	-	±2.8%
Mg	mg/kg	<1	1	<1	<1	<1	38	37	±>100%	-	±15%
Pb	mg/kg	<1	<1	<1	<1	<1	<1	<1	-	-	-
Zn	mg/kg	2	1	2	<1	<1	330	440	±44%	-	±8.6%
P	mg/kg	<1	<1	<1	<1	<1	279	266	-	-	±18%
K	mg/kg	<1	1	<1	<1	<1	5	7	±>100%	-	±20%
C	% m/m	87.51	87.93	87.13	86.02	86.29	-	-	±2.8%	±2.8%	-
H	% m/m	11.01	10.68	12.11	13.66	13.54	-	-	±6.9%	±6.3%	-
N	% m/m	0.39	0.42	0.3	<0.10	<0.10	-	-	±>100%	-	-
O	% m/m	0.35	0.44	0.34	<0.30	<0.30	-	-	±>100%	-	-
Net specific heat	MJ/kg	41.09	40.86	41.67	42.92	42.75	-	-	±1.0%	±0.9%	-

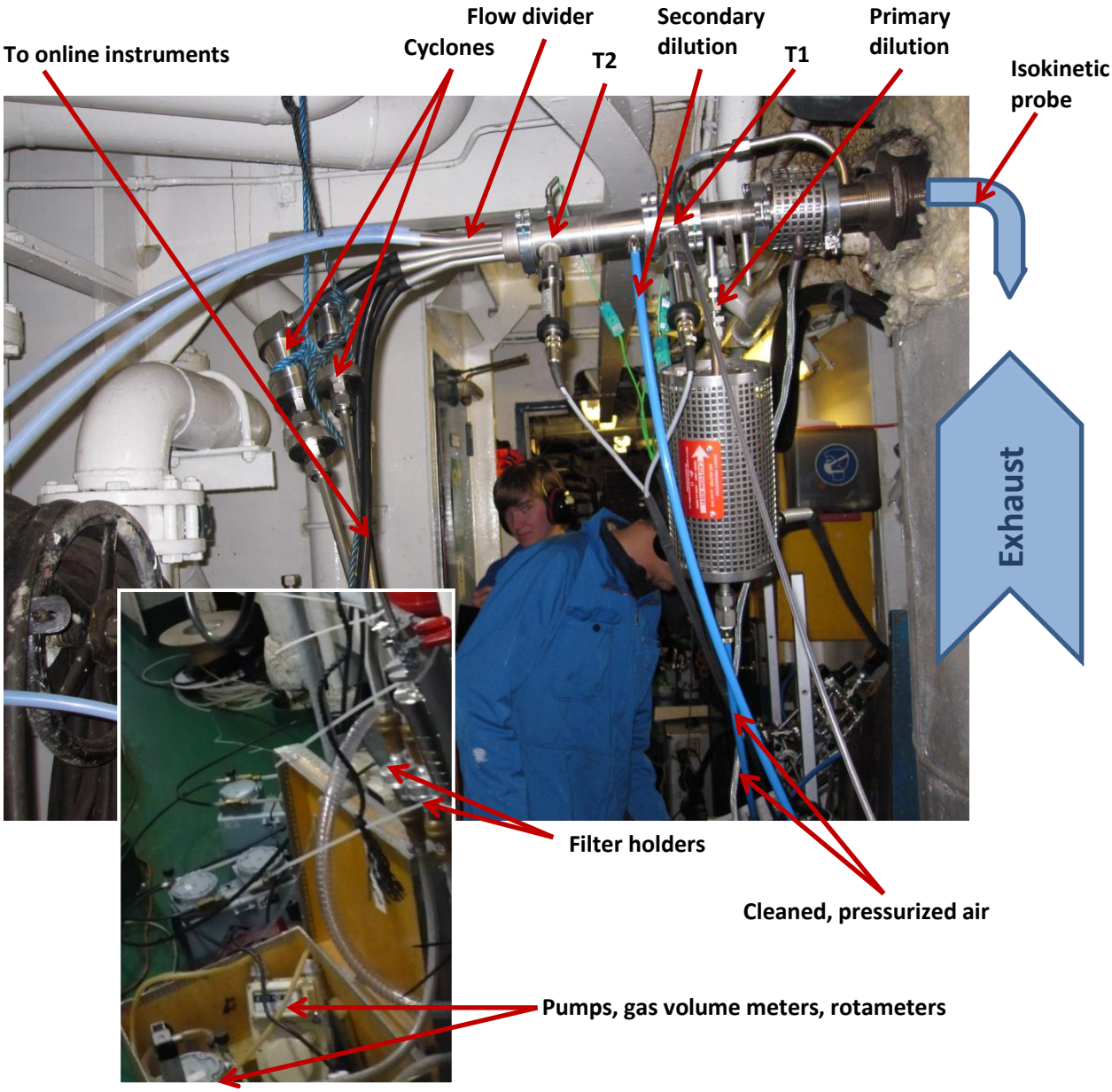

Figure S1. The measurement setup. Exhaust was sampled through an isokinetic probe to the Dekati Fine Particle Sampler (FPS-4000) (Probe to Flow divider on Figure). From the FPS the diluted and cooled exhaust was pumped through $PM_{2.5}$ and PM_{10} cyclones followed by filter holders. The vacuum pumps were connected to gas meters and rotameters for sample flow velocity and volume control. From the flow divider sample gas was also led to on-line PM instruments.

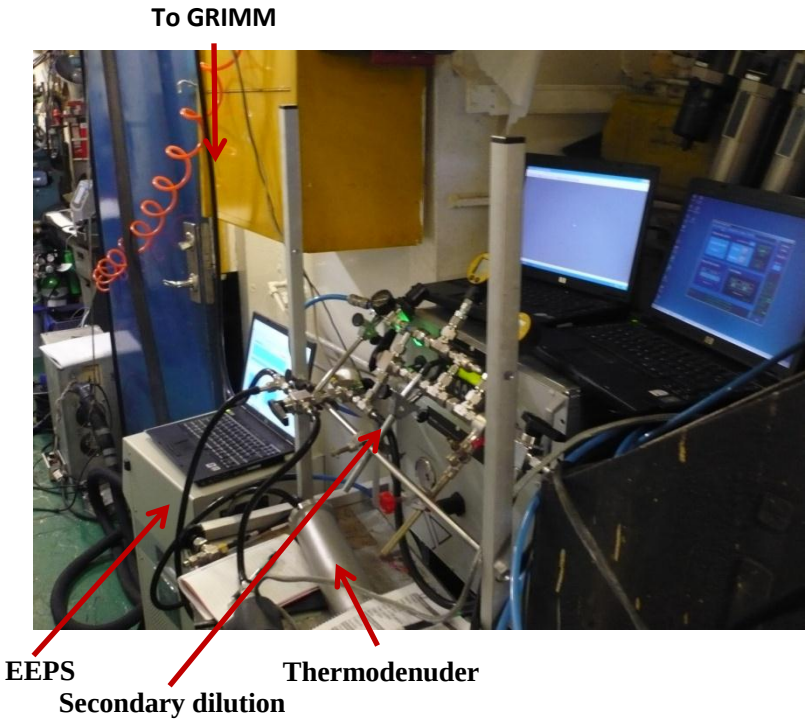

Figure S2. Setup for on-line instruments. From the FPS flow divider (Figure S1) the sample was led through secondary dilution step (Dekati DAD-100) and optionally thermodenuder to EEPS (Engine Exhaust Particle Sizer, Model 3090, TSI Inc.) and aerosol spectrometer (TSI GRIMM 1.108)

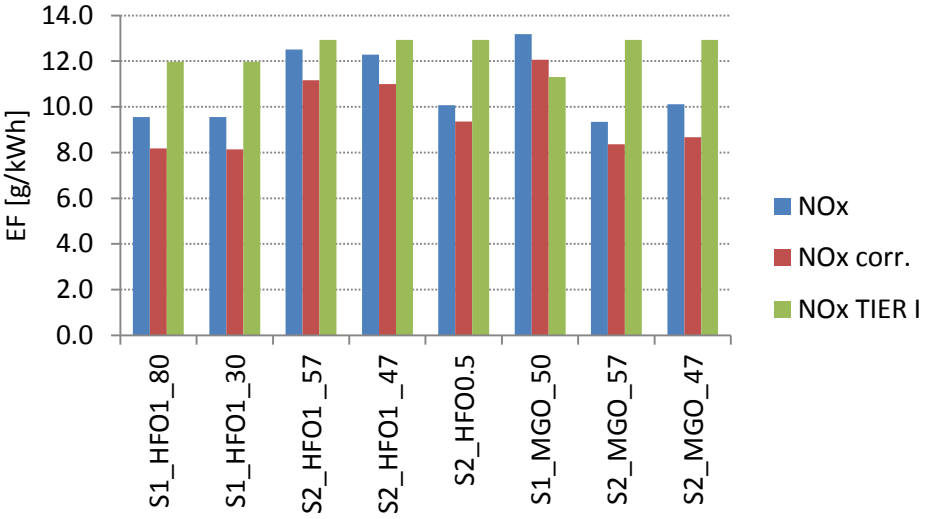

Figure S3. Emission factors for NO_X measured on investigated engines. NO_X corr. is EF(NO_X) corrected for ambient conditions (humidity and temperature) as in ISO 8178-1 1996 clause 13.3, NO_X TIER I is the maximum allowed EF(NO_X) for the engine calculated according to the TIER I NOx emission standard.

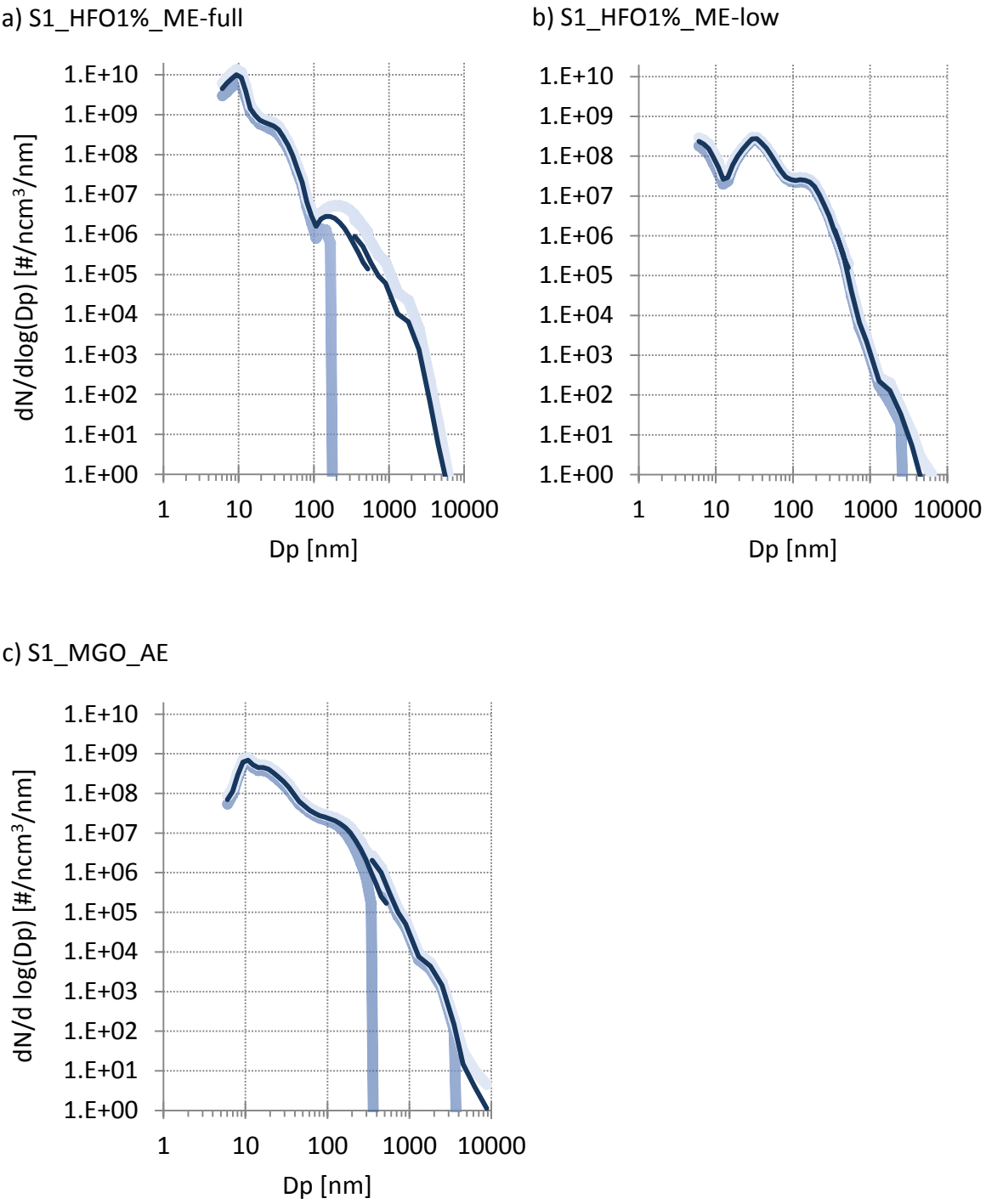

Figure S4 Particle number distributions for 3 different experiments on ship S1. The light-blue line shows 1 standard deviation interval around the mean. In size range 300-500 nm the double lines represent results from EEPS and GRIMM instruments respectively. In panel a the standard deviation for particles with Dp > 200nm is larger than Dp.

Table S4. Emission factors in [mg/kg-fuel] for elements in PM analysed by ED XRF analysis (for $SO_4^=$ and Ca+ also by IC) on filter samples. In the upper part are presented mean emission factors, in the middle part EF resulted from analyses performed in the 2 laboratories are shown. In the bottom part, mean relative uncertainties (Rel. uc. - mean uncertainty/mean concentration of a group of samples) for 4 groups of samples (S1 HFO, S1 MGO, S2 HFO, S2 MGO) are presented together with mean coefficient of variance (CV) of investigated multiple samples (2 triplets sampled in HFO exhaust).

Sample type				S	V	Ni	Fe	Cr	Mg	Al	Si	Co	K	P	Zn	Ca
S1	HFO 1%	ME-full	PM1	88.5	21.0	13.6	5.5	0.29	2.1	2.3	2.3	<d.l.	0.31	1.8	1.1	7.6
S1	HFO 1%	ME-full	PM10	34.8	20.3	13.6	5.8	0.40	5.4	3.1	2.1	<d.l.	0.05	1.0	1.1	8.3
S1	HFO 1%	ME-full	TSP	102.0	19.8	16.1	5.0	<d.l.	<d.l.	<d.l.	<d.l.	<d.l.	<d.l.	<d.l.	3.6	15.7
S1	HFO 1%	ME-low	PM1	18.1	12.6	9.6	3.3	<d.l.	<d.l.	<d.l.	<d.l.	<d.l.	<d.l.	<d.l.	0.64	2.2
S1	HFO 1%	ME-low	PM10	18.0	7.4	5.6	1.7	<d.l.	<d.l.	<d.l.	<d.l.	<d.l.	2.0	<d.l.	0.30	0.9
S1	HFO 1%	ME-low	TSP	18.0	9.9	9.2	4.3	<d.l.	<d.l.	<d.l.	<d.l.	<d.l.	2.5	<d.l.	7.6	2.4
S2	HFO 1%	ME-full	PM2.5	36.3	8.9	7.9	1.3	0.08	<d.l.	0.11	0.97	0.44	<d.l.	<d.l.	0.35	2.3
S2	HFO 1%	ME-full	PM10	37.6	8.5	8.1	1.4	0.13	0.9	0.97	0.22	0.35	<d.l.	<d.l.	0.24	2.1
S2	HFO 0.5%	ME-full	PM2.5	22.6	2.3	5.7	0.65	0.09	0.3	0.45	<d.l.	0.35	<d.l.	<d.l.	0.35	1.6
S2	HFO 0.5%	ME-full	PM10	28.5	2.5	6.3	0.91	<d.l.	1.0	0.97	<d.l.	0.26	<d.l.	<d.l.	0.16	1.9
S2	MGO	ME-full	PM2.5	1.1	0.21	<d.l.	0.048	0.02	<d.l.	<d.l.	0.28	<d.l.	<d.l.	<d.l.	<d.l.	1.3
S2	MGO	ME-full	PM10	1.6	0.17	0.068	0.052	0.11	<d.l.	<d.l.	0.14	<d.l.	<d.l.	<d.l.	0.24	1.3
S1	MGO	AE	PM1	2.4	0.007	0.015	0.098	0.17	2.8	0.97	0.16	<d.l.	<bl.	0.047	1.2	7.8
S1	MGO	AE	PM10	2.6	0.007	0.015	0.098	0.17	<d.l.	<d.l.	<d.l.	<d.l.	<d.l.	<d.l.	1.4	9.5
S1	MGO	AE	TSP	2.7	<d.l.	<d.l.	<d.l.	<d.l.	<d.l.	<d.l.	<d.l.	<d.l.	<d.l.	<d.l.	1.7	11.2
S1	HFO 1%	Lab1	PM2.5	66.9	18.0	13.8	5.3	<d.l.	-	-	-	0.6	<d.l.	-	1.1	5.6
S1	HFO 1%	Lab 2	PM2.5	78.3	23.9	13.5	5.7	0.3	2.1	2.3	2.3	0.7	0.3	1.8	1.0	9.6
S1	HFO 1%	Lab 1	PM10	23.7	20.1	14.9	5.7	<d.l.	-	-	-	0.6	<d.l.	-	1.3	7.2
S1	HFO 1%	Lab 2	PM10	45.8	20.6	12.3	5.9	0.4	5.4	3.1	2.1	0.6	0.1	1.0	0.8	9.4
S1	MGO	Lab 1	PM2.5	<d.l.	<d.l.	<d.l.	<b.v.	<d.l.	-	-	-	<d.l.	<d.l.	-	1.4	7.3
S1	MGO	Lab 2	PM2.5	2.3	0.007	0.015	0.20	0.17	2.8	1.0	0.16	<b.v.	<b.v.	0.047	0.9	8.4
S1	Rel. uc.	HFO 1%		3.6%	3.8%	3.7%	4.0%	42.9%	17.9%	9.9%	8.8%	11.1%	-	11.9%	14.1%	5.3%
S2	Rel. uc.	HFO 1%, 0.5%		3.6%	5.5%	4.1%	12.5%	>100%	45.7%	44.0%	25.6%	20.8%	-	-	37.6%	11.0%
S1	Rel. uc.	MGO		4.2%	-	-	20.5%	40.8%	13.0%	14.0%	52.0%	-	-	>100%	7.7%	4.5%
S2	Rel. uc.	MGO		5.0%	48.1%	87.1%	>100%	>100%	-	-	43.3%	-	-	-	41.5%	14.1%
S1, S2	Mean CV	HFO 1%		15.2%	12.2%	10.1%	14.9%	78.5%	47.1%	31.8%	19.0%	20.1%	141.4%	19.3%	31.4%	16.8%

Table S5. Sample Pearson correlation coefficients r for emission factors for elements measured by the ED XRF analysis on filter samples and for EF(PM-mass) measured on the same samples. Three groups with high correlation are marked with different colours.

	S	V	Ni	Fe	Cr	Mg	Al	Si	Co	Zn	Ca	PM
S	1	0.752	0.773	0.628	0.493	0.013	0.441	0.802	0.436	-0.056	0.331	0.683
V		1	0.947	0.958	0.784	0.587	0.804	0.947	0.703	0.470	0.500	0.899
Ni			1	0.908	0.617	0.393	0.697	0.882	0.558	0.449	0.397	0.925
Fe				1	0.863	0.662	0.905	0.961	0.449	0.490	0.537	0.876
Cr					1	0.902	0.986	0.804		0.604	0.747	0.696
Mg						1	0.847	0.500		0.755	0.834	0.442
Al							1	0.765	-0.843	0.674	0.773	0.703
Si								1		0.555	0.652	0.869
Co									1	0.863	0.500	0.473
Zn										1	0.946	0.383
Ca											1	0.301

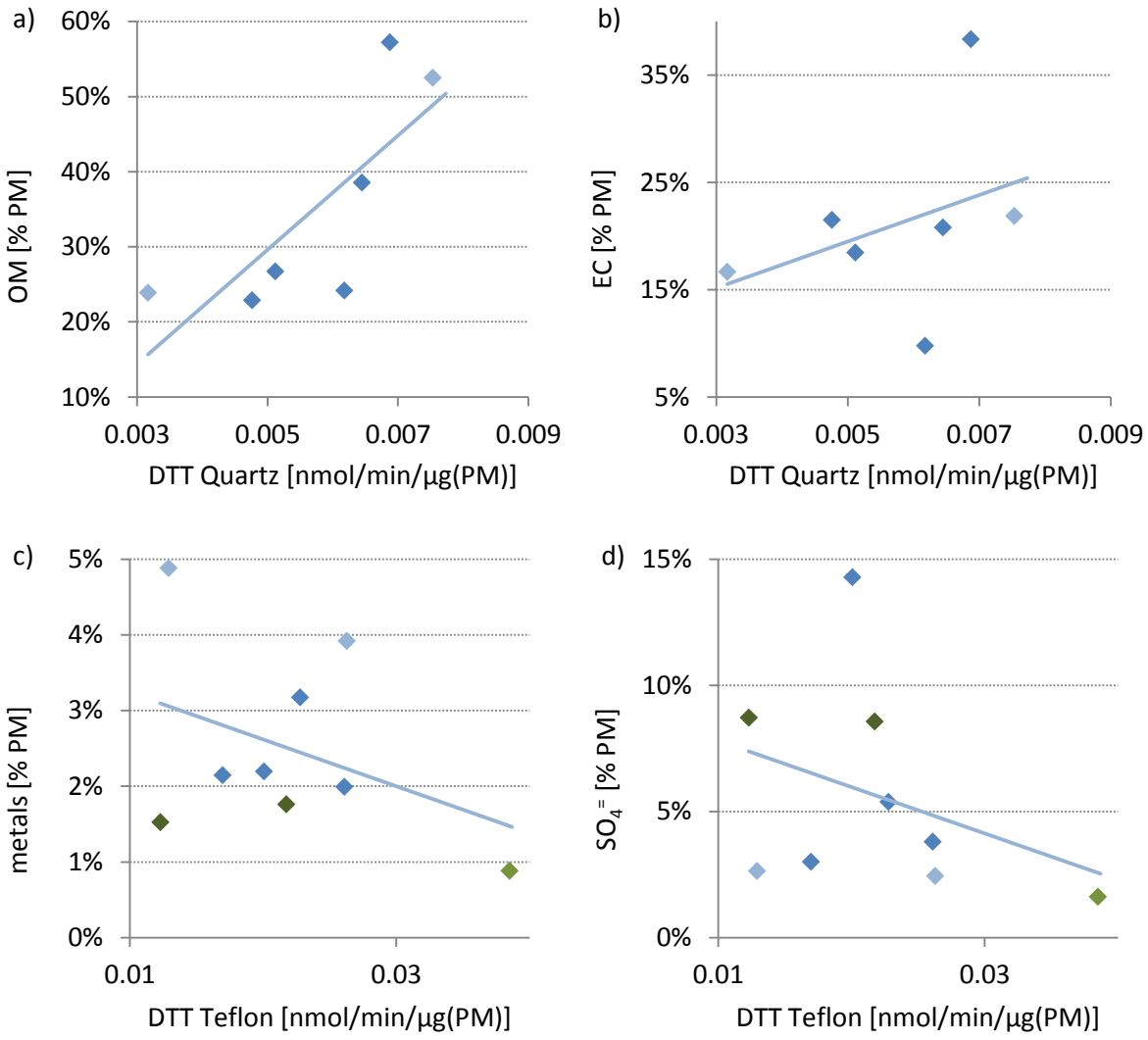

Figure S5. Plots of relative contributions of PM compounds to PM mass (in wt%) against oxidative potential measured on quartz (a, b) and Teflon (c, d) filters. a – OM, b – BC, c – metals analysed with XRF, d – sulphate calculated from S analysed by XRF. Color coding of points: dark blue – HFO fuel, S1, light blue – MGO fuel S1, dark green – HFO fuels S2, light green – MGO fuel S2.

a)

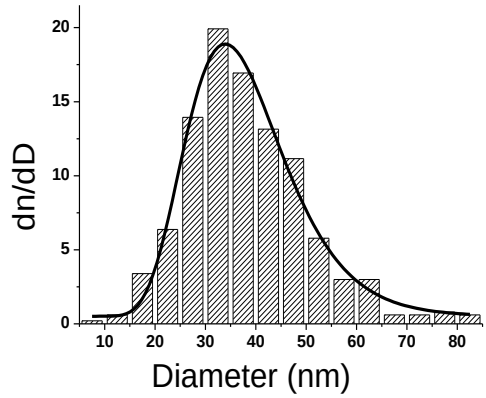

b)

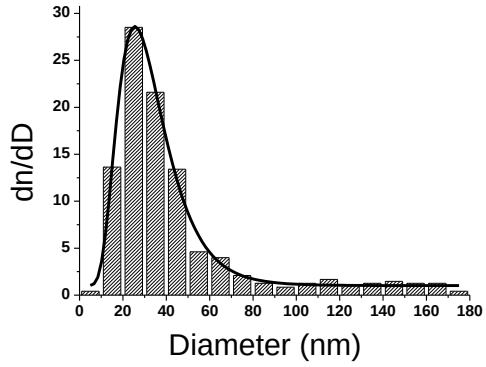

Figure S6. Size distribution of primary soot-type particle and its longnormal fit (solid line) for a – S1_HFO1%_ME-full experiment (based on 502 images) and b – S1_MGO_AE experiment (based on 477 images)

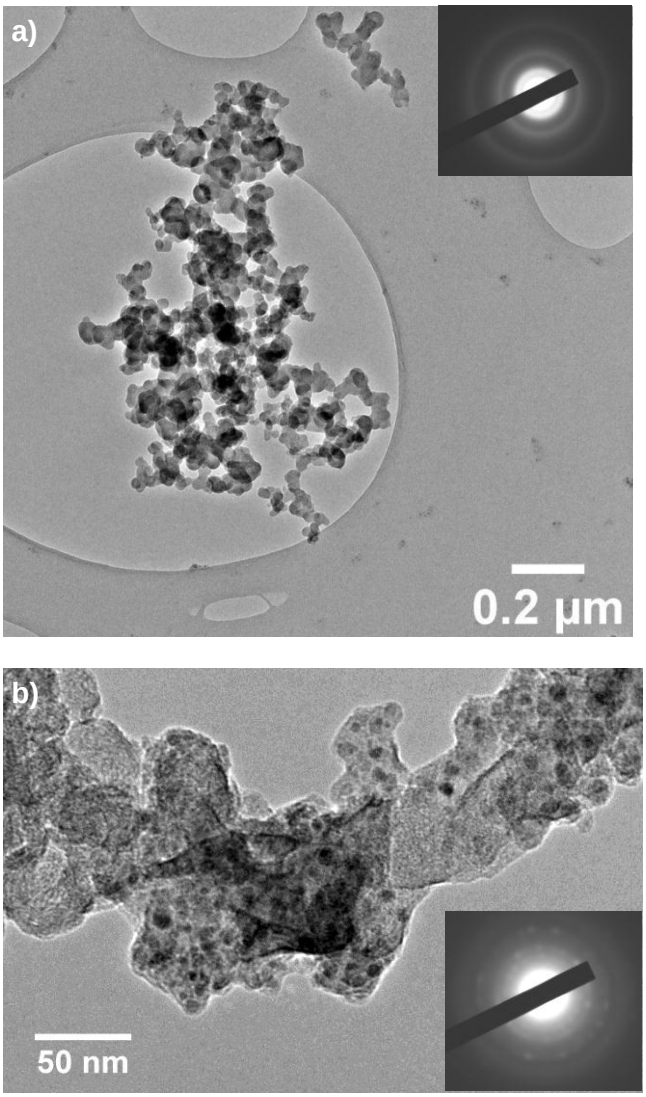

Figure S7. a - TEM picture of a small soot-type aggregate and its corresponding SAED pattern, b - zoom on soot-type particles with dark dots and its associated SAED pattern

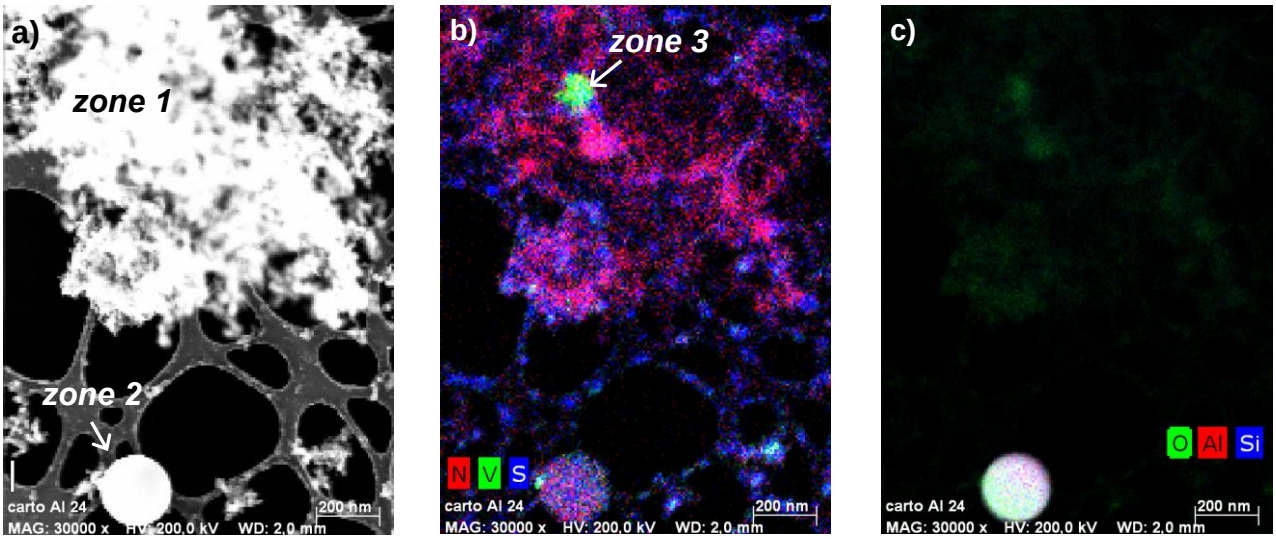

Figure S8. a – STEM image of an agglomerate of soot-type particles (zone 1, composition: C - 84.0 wt%, O - 5.4 wt%, and N - 13.3 wt%, traces <0.1 wt% V, Ni, S and Si) and char-mineral particle (zone 2, composition: O - 58.7 wt%, Al - 24.5 wt%, Si - 16.8 wt%) from the S1_HFO1%_ME-full experiment. b, c – Elemental composition map for V, N, and S (b) and for O, Al and Si (c) of particles on image a. Zone 3 in image b is a particle dominated by V with 14.6 wt% of O and traces of Ca, S and Ni.

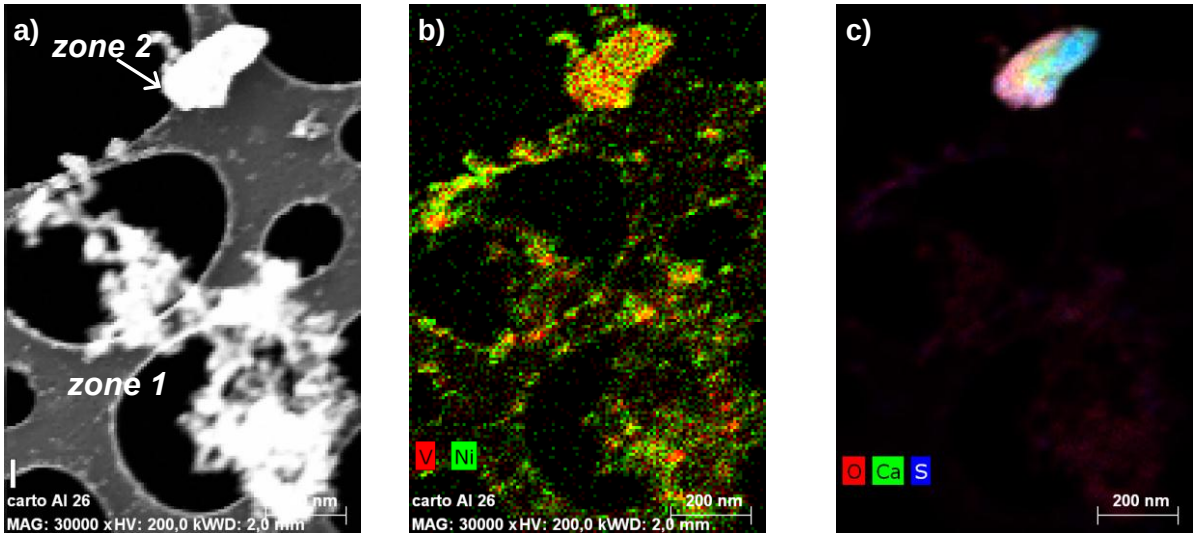

Figure S9. a – STEM image of a soot agglomerate (zone 1) and a char-mineral particle (zone 2) from the S1_HFO1%_ME-full experiment. Composition of the soot agglomerate: C 76.8 wt%, N 17.2 wt%, O 5.9 wt%, traces of V, Ca and S (about 0.1 wt% of each element). b, c – Elemental composition map for V and Ni (b) and for O, Ca and S (c) of particles in a.

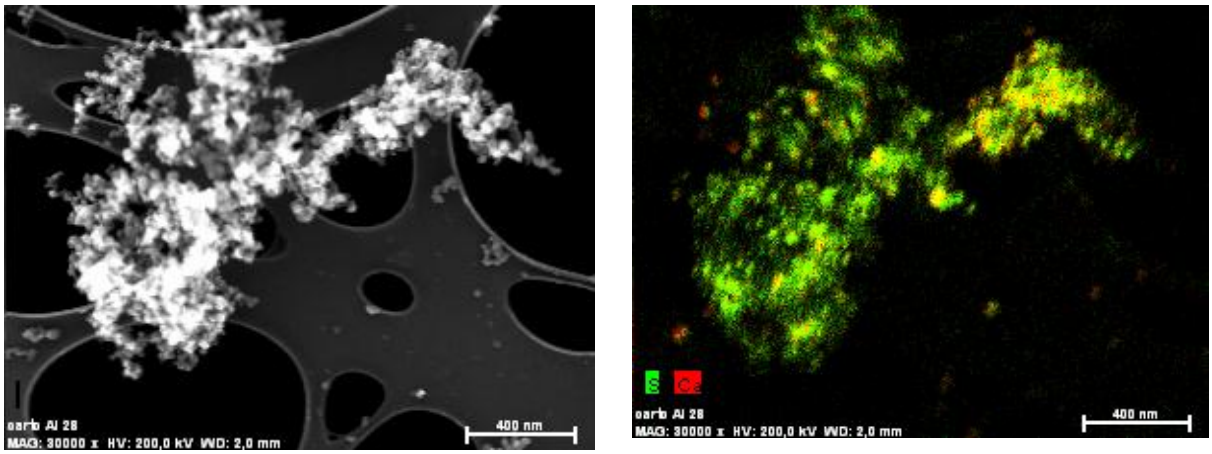

Figure S10. a – STEM image of a soot agglomerate collected in S1_MGO_AE experiment. b – Elemental composition map for Ca, and S of the soot agglomerate in a.

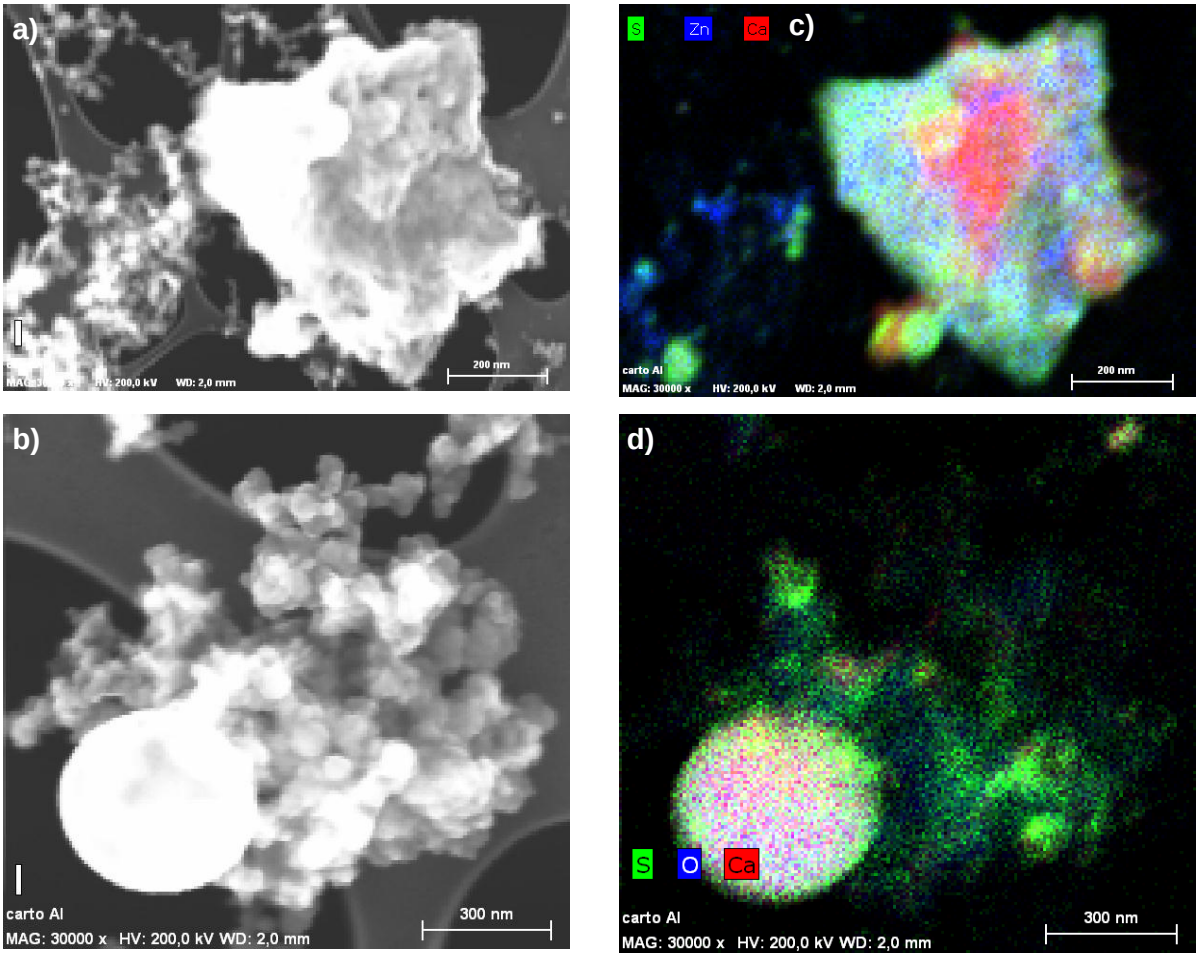

Figure S11. a, b – STEM image of char-mineral particle and soot particles collected in S1_MGO_AE experiment. Composition of the char-mineral particle in a: C 66.5 wt%, O 24.8 wt%, Ca 7.8 wt%, S 0.7 wt%, P 0.2 wt%; Composition of the char-mineral particle in b: C 73.3wt%, O 24.3 wt%, Ca 2.1 wt%, S 0.3 wt%. c – elemental composition map for Ca, S and Zn of particles in a. d – elemental composition map for Ca, S and O of particles in b.

a) b)

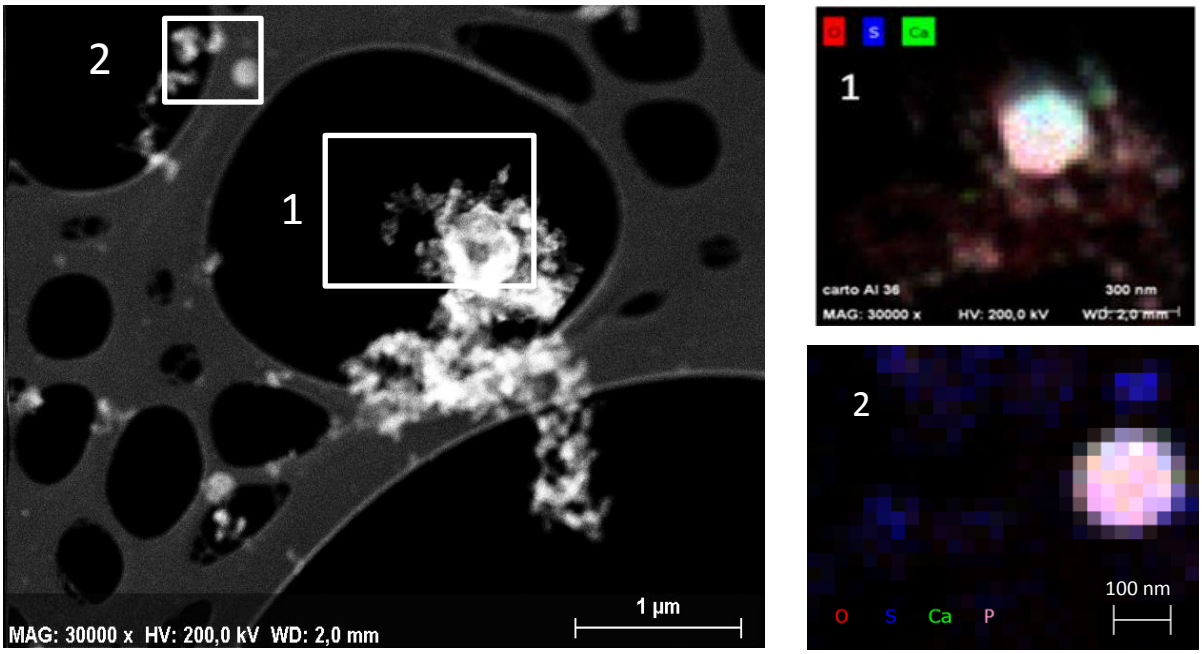

Figure S12. a - STEM image of soot agglomerates with a large (~500 nm) char-mineral particle (zone 1) and smaller char-mineral particle (zone 2). Composition of char-mineral particle in zone 1: C 58.4 wt%, O 35.1 wt%, Ca 3.7 wt%, S 2.8 wt%; composition in zone 2: C 51.7 wt%, O 39.8 wt%, Ca 5.6 wt%, P 2.9 wt% and S 0.1 wt% the small particles have traces of S only. b - Elemental composition map corresponding to the zone 1 (O, S, Ca) and zone 2 (O, S, Ca, P) in figure 4a.

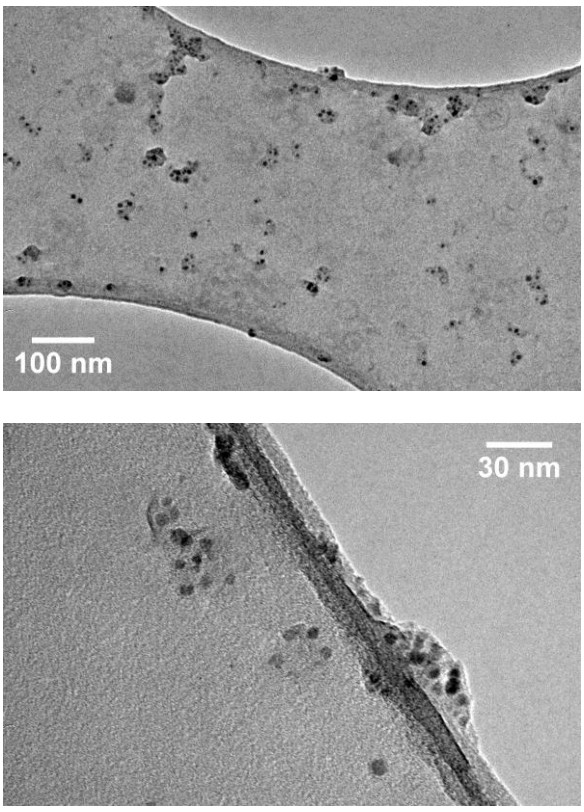

Figure S13. TEM image of organic particles.

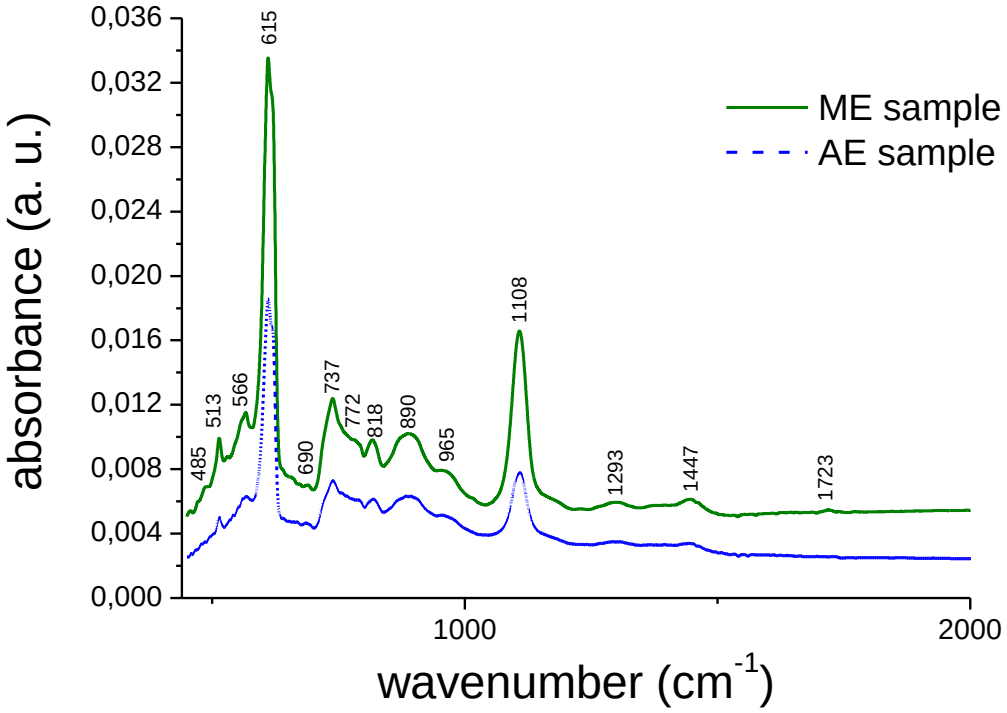

Figure S14. FTIR spectra of auxiliary engine (AE) and main engine (ME) particulate matter samples Peaks at 485 and 818 cm^{-1} are linked to the presence of aromatic ring vibrations, medium peaks at 737, 772, 818, 890 cm^{-1} to C-H out of plane vibrations in aromatics compounds (Socrates, 2004). A weak peak at 1723 cm^{-1} is probably due to C=O in ketone, ester, anhydride or aldehyde (DEAN'S, 2004). Medium peaks at 513 and 965 cm^{-1} are due to V-O vibration of the vanadium oxide V_2O_5 (Botto et al., 1997, Clauws et al., 1985), medium peak at 566 cm^{-1} and its shoulder at 558 cm^{-1} come from Fe-O vibration of the iron oxide Fe_3O_4 (Namduri et al., 2008). The very strong peak at 615 cm^{-1}, its shoulder at 620 cm^{-1} and a weak peak at 690 cm^{-1} come from the C-S stretching of sulphide compounds (DEAN'S, 2004). The very strong peak at 1108 cm^{-1} indicates the symmetric stretch of SO_2 in sulfone, C=S vibrations of thiocarbonyl compounds or C-O-C asymmetric stretch (DEAN'S 2004; Socrates, 2004). A weak peak at 1293 cm^{-1} are probably linked to C-N stretching in aromatic aryl-NH_2 compounds (DEAN'S, 2004). A weak peak at 1447 cm^{-1} can correspond to C-N-H bending in amide compounds (DEAN'S, 2004) or ammonium ion NH_4^+ (Maria et al., 2002).

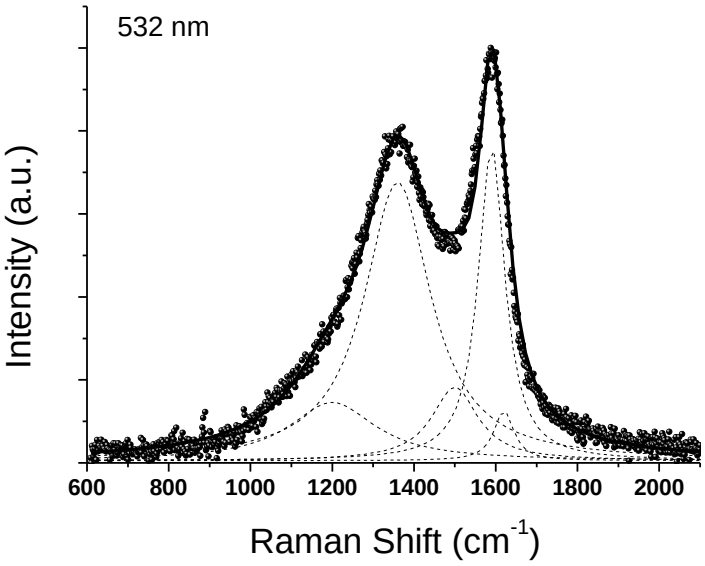

Figure S15. Raman spectra of the cumulative S1_MGO1%_ME sample. Five bands are identified (Sadezky et al., 2005): G, D_1, D_2, D_3, and D_4. The G band (1580 cm^{-1}) corresponds to the E_{2g} symmetry mode of the graphite lattice. The D_1 band (1350 cm^{-1}) originates from A_{1g} symmetry mode in disordered graphite; D2 band (1620 cm^{-1}) - from E_{2g} symmetry stretching mode of disordered graphite; D_3 band (1500 cm^{-1}) is related to amorphous carbon (a mixture of sp^2 and sp^3); and D_4 band (1200 cm^{-1}) is assigned to A_{1g} symmetry mode of disordered graphite.